Substitution of carbon black with wood biochar in natural rubber composites: A study on reinforcement and sustainability

Virág Á. D., Görbe Á., Kohári A., Tóth Cs.

Results in Engineering 28 (2025) 107843

Contents lists available at ScienceDirect

Results in Engineering

journal homepage: www.sciencedirect.com/journal/results-in-engineering

Substitution of carbon black with wood biochar in natural rubber composites: A study on reinforcement and sustainability

Ábris Dávid Virág [a], Ákos Görbe [a], Andrea Kohári [a], Csenge Tóth [a,b,*]

[a] Department of Polymer Engineering, Faculty of Mechanical Engineering, Budapest University of Technology and Economics, Műegyetem rkp. 3., H-1111 Budapest, Hungary

[b] MTA-BME Lendület Lightweight Polymer Composites Research Group, Budapest University of Technology and Economics, Műegyetem rkp. 3., H-1111 Budapest, Hungary

ARTICLE INFO

Keywords:
Rubber production
Energy demand
CO_2 Emission
Mechanical properties
Microstructure
Elastomer
Carbon footprint

ABSTRACT

The increasing demand for sustainable materials in the rubber industry has prompted the search for renewable alternatives to carbon black (CB). Biochar (BC), a carbon-rich byproduct of biomass pyrolysis, offers a promising solution. In this study, we investigate the substitution of CB with wood-based BC at different ratios in natural rubber (NR) composites, and we evaluate its effect on mechanical properties, processability, and environmental performance. To assess sustainability, we quantified CO_2 emissions and energy requirements based on material inputs and processing parameters during the mixing and curing stages. With increasing BC contents, tensile strength, strain at break and modulus at 300 % strain decreased linearly. However, the initial tensile stiffness increased indicating that BC-filled NR composites may be advantageous for applications under small deformations. Higher BC contents also led to higher viscosity, which increases the energy requirements for processing. Overall, at a BC content of 20 %, tensile strength, modulus at 300 % strain and strain at break was reduced by 13 % (from 24.3 to 31.1 MPa), 16 % (from 12.6 to 10.6 MPa) and 3.6 % (from 500 % to 482 %), respectively, while CO_2 emissions were reduced by 20 % and energy requirements remained low. The results indicate that integrating BC as a partial substitute for CB can help reduce environmental impact while maintaining satisfactory rubber performance.

1. Introduction

The automotive industry is the largest consumer of carbon black (CB), accounting for approximately 70 % of global production [1]. CB production is highly energy-intensive, contributes substantially to CO_2 emissions, and poses notable health and environmental risks [2]. However, CB is crucial for rubber production due to its exceptional reinforcing properties, as CB significantly enhances the mechanical strength, durability, and wear resistance of rubber compounds [1,3]. Therefore, numerous studies in the literature have focused on making both carbon black and rubber production more sustainable [4–6]. Rosner et al. [7] developed a detailed process and economic model of a carbon black plant to evaluate mass and energy balances, CO_2 emissions, and the viability of tail gas utilization strategies. They conclude that current processes remain highly CO_2-intensive and polluting, which highlights the need for new, sustainable production methods, or alternative replacements. Methods are emerging to make CB production more sustainable. Wu et al. [8] propose an integrated process that combines waste tyre pyrolysis with carbon black production to address the environmental and resource challenges of conventional CB manufacturing, which heavily depends on fossil feedstocks and energy. The authors derived pyrolytic oil from end-of-life tyre pyrolysis to replace both the petroleum and natural gas required in CB production. Life cycle assessment results show that feedstock oil in conventional CB production contributes over 30 % of the total environmental impact. They proved that their method decreased the energy demand of the process. Recycled CB also has great potential to decrease the environmental burden of rubber production [9]. Sagar et al. [10] investigated the use of recycled carbon black (rCB) derived from the pyrolysis of end-of-life tyres as a filler in ethylene propylene diene (EPDM) rubbers. The authors found that rCB particles were smaller than conventional N550 carbon black particles, had higher ash content, and contained impurities such as silica, sulphur and zinc oxide. These factors led to reduced cure characteristics, lower crosslink density, and inferior

* Corresponding author.
E-mail address: tothcs@pt.bme.hu (C. Tóth).

https://doi.org/10.1016/j.rineng.2025.107843
Received 10 August 2025; Received in revised form 8 October 2025; Accepted 19 October 2025
Available online 19 October 2025

mechanical properties compared to N550. Dwivedi et al. [11] also applied rCB sourced from waste tyre pyrolysis in NR composites. Although rCB-filled NR composites showed improved tensile strength and elongation at break, they had reduced tensile modulus, tear strength and compression set, which were attributed to poor interaction between the rCB particles and the rubber matrix. The authors concluded that rCB is suitable for partial substitution of CB.

Still, there is increasing interest in developing more sustainable alternatives [12]. Biochar (BC) is appearing in more and more research as an alternative to carbon black [13]. BC is produced by the pyrolysis of organic biomass from agricultural waste, wood chips or manure. The chemical composition, microstructure, and mechanical properties of BC depend largely on the type of feedstock used and the specific conditions of the pyrolysis process [14]. BC is also gaining popularity due to its potential in CO_2 removal [15]. When produced under the right conditions, BC can be carbon neutral, meaning the CO_2 emitted during its production and application is balanced by the CO_2 absorbed by the biomass it originates from. Even more beneficially, BC can be carbon negative when its production captures more carbon than it emits [16]. Kane et al. [17] used a compositional LCA model combined with scenario-based Monte Carlo simulations to evaluate the carbon dioxide removal potential of BC. The authors found that in the best-practice case, BC production achieves a median cradle-to-gate carbon dioxide removal of 1.4 kg carbon dioxide equivalent per kg (CO_2e/kg) biomass. In contrast, the poor-practice case yields median net emissions of 0.090 kg CO_2e/kg.

Rice husk biochar typically has a high silica content and a porous, brittle structure, which can make it more abrasive and less reinforcing in polymer matrices [18,19]. In contrast, wood biochar has a carbon-rich structure with higher surface area, often resulting in better compatibility and dispersion [20–22]. Chicken manure biochar is rich in nutrients and minerals, has a high ash content, and tends to have a more irregular, compact structure [23,24]. Unlike many other agricultural residues, pistachio shells produce biochar with a high carbon content (>80 %) and low ash content (<5 %), characteristics critical for maintaining mechanical performance [25]. BC produced from lignin exhibits a highly structured morphology consisting of primary nanoparticles that aggregate into irregular, large-surface fragments. After high-temperature carbonization, lignin BC exhibits a specific surface area of 83 m^2/g and a mesoporous structure. The carbonization process removes most oxygen-containing groups, resulting in a more hydrophobic, graphite-like structure that improves compatibility with rubber matrices [26]. Biochar produced from oat straw through pyrolysis at 600 °C had a high carbon content and a fine particle size and was found to have good dispersion in rubber matrices [27]. Corn-based biochar produced from corn cob, corn stover, and corn starch feedstocks exhibit larger and irregular aggregates, a wide particle size distribution, and polar surface chemistry due to lower carbon and higher oxygen/-hydrogen content. Corn-based BC was found applicable as semi-reinforcing filler in styrene-butadiene rubber (SBR) due to its physicochemical similarities to N772 CB [28].

In research, various types of BCs were added to rubber compounds to replace carbon black. Sittitanadol et al. [29] investigated the use of biochar derived from different parts of coconut waste. Their results show that the high-carbon coconut biochar provided effective reinforcement, significantly improving Shore A hardness, tensile modulus, and tensile strength, especially at a filler content of 40 phr. Lubura et al. [30] compared the effects of biochar from hardwood waste with conventional CB as fillers in rubber composites, focusing on energy consumption, vulcanization behaviour, and mechanical properties. Using filler contents ranging from 0 to 50 phr, they found that up to 20 phr, both fillers showed comparable electricity consumption during mixing, but higher CB content significantly increased energy demand. The study concluded that biochar could effectively replace CB up to 30 phr while maintaining similar performance. Sunali et al. [31] conducted a study on NR composites reinforced with biochar derived from bamboo waste. The addition of BC at 10 and 20 phr increased thermal stability and conductivity, and improved mechanical performance. The study concluded that the biochar composites are promising eco-friendly alternatives to conventional fillers for vibration and noise control applications. Peterson and Chisholm [25] used pistachio shell biochar as a partial replacement for carbon black in NR composites. They tested fillers consisting of a mixture of pistachio shell BC and CB to determine the maximum substitution level before the composite integrity deteriorated. Up to 40 % of the CB can be replaced with pistachio shell BC without any deterioration in performance; in fact, the tensile strength, elongation at break, and toughness of the rubber improved. However, this replacement led to a decrease in stiffness. Miedzianowska-Masłowska et al. [32] investigated the use of bio-based fillers—biomass, phyto-ash, and biochar produced from beech wood—in NR composites. They found that biochar and biomass fillers at 30 phr significantly increased hardness, stiffness, and crosslink density, with biochar producing the highest tensile strength. Jiang et al. [33] investigated the use of lignin-derived biochar as a renewable reinforcing filler in SBR composites. When mixed into SBR at a concentration of 40 phr, BC improved tensile strength and elongation at break. Miedzianowska-Masłowska et al. [27] investigated BC obtained from oat straw as a renewable filler in NR composites. Compared to CB, BC improved cross-linking and tensile strength, but the vulcanizates showed lower aging resistance due to oxidation by heat. Abidin et al. [34] investigated the potential of palm kernel shell biochar BC derived from palm oil industry waste as a sustainable alternative to CB. Their results showed that increasing BC content reduced cure time and enhanced cure rate, while maintaining abrasion resistance and hardness. Bardha et al. [35] applied nutshell and grain husk waste BC as fillers for styrene-butadiene rubber composites. The authors showed that biochars provided reinforcement with mechanical performance comparable to CB. They also applied a slurry-based activation which further enhanced the mechanical properties of the composites. Lubura et al. [36] investigated the use of hydrochar (HC), a biomass-based filler derived from the hydrothermal carbonization of hardwood sawdust as a partial replacement of CB in NR composites. Rubber composites with varying HC/CB ratios (up to 40/10 phr) showed good filler dispersion and no defects after vulcanization. The study concludes that replacing 10–20 phr of CB with HC is viable.

While BC has emerged as a promising, renewable alternative to CB in rubber composites, its properties vary significantly depending on its source and the parameters of pyrolysis, affecting its reinforcing behaviour. Most studies using BC highlight trade-offs such as reduced aging resistance or lower modulus. At the same time, the environmental impact of rubber production and filler selection is often overlooked. Full substitution of CB with BC often leads to a deterioration in mechanical properties but since BC is proven to reduce environmental impacts, an optimal balance should be found between sustainability and performance. Wood biochar is generally rich in carbon, porous, and hydrophobic in structure, compared to biochar produced from many agricultural wastes. It typically contains less ash and minerals, provides a larger surface area and porosity for polymer infiltration, and has less polar surface chemistry. These properties make wood biochar a potentially effective reinforcing filler in composite systems. We investigated the possibility of partially or fully replacing CB with BC produced from wood waste with different filler contents. We evaluated the effect of BC on the most important mechanical properties and processability of NR composites and also analysed how different biochar contents influence the environmental footprint of the composites, with a particular focus on carbon emission and the energy requirements of the manufacturing process of NR.

2. Materials and sample preparation

2.1. Preparation of biochar filler

Biochar was supplied by Explocom GK SRL (Cristuru Secuiesc,

Romania). The material composition of the wood-based biochar is shown in Table 1. As received, the biochar particles were approximately 1 cm^3 in size (Fig. 1a). Their size was first reduced using a coffee grinder, after which a CISA BA 200 N sieve shaker (CISA Cedaceria Industrial, Barcelona Spain) was employed to separate them into fractions. Particles measuring 75 μm or less were used for the rubber mixtures (Figure 1/b). The particle size distribution of the biochar used in this study reflects laboratory-scale production and milling conditions, which may differ from those of industrially produced feedstocks. Variations in grinding and sieving processes could lead to differences in particle size and morphology.

2.2. Rubber formulations and mixing

A general-purpose natural rubber (NR), SMR CV 60 (Akrochem Corp; Akron, OH, USA; Mooney viscosity (ML, 1 + 4, 100°C): 55–65) and different additives were used for the compounds (Table 2).

The rubber compounds were prepared with a Brabender Lab-Station internal mixer (Brabender GmbH & Co. KG, Duisburg, Germany)) equipped with a W 350 E chamber (free volume 370 cm^3). The temperature was set to 60°C, and the batches were mixed at 40 rpm. Then, to increase homogeneity, we passed the mixtures through an LRM-SC-110/T3E (Labtech Engineering Co., Ltd., Thailand, Samutprakarn) two-roll mill. The recipes can be found in Table 2. We examined the gradual substitution of carbon black (CB) with biochar (BC). Therefore, in the denominations, "BC" refers to biochar, and the number indicates the percentage of BC added as a replacement to CB. The quantity of CB in BC0 is the base value (100 % CB). Therefore, for example in the case of BC20, 20 % of the total quantity of CB was replaced with BC (Table 3). In accordance with previous results [37], soybean oil was used as a sustainable plasticizer to improve the processability of the rubber compounds.

We made 160 mm x 160 mm rubber sheets of the flattened compounds by compression moulding at 160℃ with a Teach-Line Platen Press 200E (Dr. Collin GmbH, Munich, Germany) machine using 2-mm mm-thick steel press frames. The sheets were pressed at 20 MPa (pressure on the sample surface was 2.5 MPa). Pressing time was determined according to the vulcanization time (t_{90}) of each compound. Then, the sheets were cooled down with water cooling of the press plates and removed from the press when the temperature of the mould reached 60°C. The specimens were punched from these sheets with standardized dies.

Table 1
Material composition of the wood biochar (data supplied by the manufacturer).

Property	Value	Unit of measurement
Bulk density < 3 mm	276	kg/m^3
Brunauer–Emmett–Teller specific surface area	557.8	m^2/g
Water holding capacity	162.5	%
Ash content (550°C)	4.1	% (w/w)
Carbon (organic)	91.3	% (w/w)
Nitrogen [N]	0.66	% (w/w)
Sulfur [S]	0.03	% (w/w)
Lead [Pb]	<2	mg/kg
Cadmium [Cd]	<0.2	mg/kg
Copper [Cu]	5	mg/kg
Nickel [Ni]	4	mg/kg
Mercury [Hg]	<0.07	mg/kg
Zinc [Zn]	15	mg/kg
Chromium [Cr]	1	mg/kg
Boron [B]	15	mg/kg
Manganese [Mn]	328	mg/kg

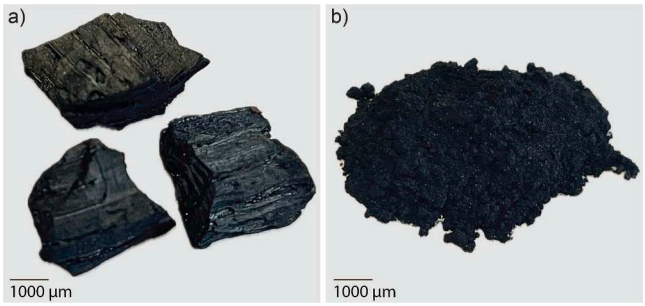

Fig. 1. Wood biochar a) as-received particles, b) sieved particles measuring 75 μm or less used as filler.

Table 2
Materials for the rubber formulations.

Material	Manufacturer	Trademark	Function
Zinc oxide (ZnO)	Werco Metal (Zlatna, Romania)	-	Activator
Stearic acid	Oleon (Ertvelde, Belgium)	Radiacid 0154	Activator
N-cyclohexyl-2-benzothiazolesulfenamide (CBS)	Rhein Chemie (Mannheim, Germany	Rhenogran CBS-80	Accelerator
Sulphur	Ningbo Actmix Polymer (Ningbo, Zhejiang, China)	ACTMIX S-80	Curing agent
Soybean oil	Vandamme Hungary Ltd. (Komárom, Hungary)	Degummed non-GMO	Processing oil
N772 carbon black (CB)	Omsk Carbon Group (Omsk, Russia)	-	Filler
Biochar (BC)	Explocom GK SRL (Cristuru Secuiesc, Romania)	-	Filler

Table 3
Rubber formulations with different biochar (BC) content.

	Amount of ingredients (phr)					
	BC0	BC20	BC40	BC60	BC80	BC100
NR-CV60	100	100	100	100	100	100
Carbon Black (CB)	50	40	30	20	10	0
Biochar (BC)	0	10	20	30	40	50
Soybean oil	5	5	5	5	5	5
ZnO	5	5	5	5	5	5
Stearic acid	2	2	2	2	2	2
CBS	1.5	1.5	1.5	1.5	1.5	1.5
Sulphur	1.5	1.5	1.5	1.5	1.5	1.5

3. Test methods

3.1. Microstructure

Scanning Electron Microscope (SEM) images of the biochar particles were taken with a JSM 6380LA scanning electron microscope from Jeol Ltd. (Japan). The samples were sputtered with gold using a Jeol JPC1200 cathodic sputtering gold plating apparatus (Jeol Ltd., Tokyo, Japan) to eliminate static charging. Size measurements were acquired with ImageJ. Sieved biochar particles with particle size 75 μm or less were mapped using scanning electron microscopy with energy

dispersive spectrometry (SEM-EDS) at 100x magnification.

3.2. Rheological and vulcanization characteristics

The curing properties of the rubber compounds were examined with a MonTech D-RPA 3000 (MonTech (Buchen, Germany)) rubber process analyser. We characterized vulcanization at 160°C (1.67 Hz and 1° amplitude) for 15 min and calculated the main parameters of the vulcanization process. Scorch time (t_{s2}) was calculated as the time it takes for the torque to increase by two units (dNm) above the minimum torque (S'_{min}), and vulcanization time (t_{90}) was determined as the time to reach 90 % curing. We also determined the difference between the maximum (S'_{max}) and minimum (S'_{min}) of the torque curve. Three measurements were performed in each case.

The Mooney viscosity of the rubber compounds was examined with a MonTech MV 3000 (MonTech (Buchen, Germany)) Mooney viscosimeter. Viscosity was characterized with a 10 mm rotor (2 rpm, 100°C) for 6 minutes (1 minute preheat, 4 minutes measurement, 1 minute relaxation). The ML 1+4 Mooney viscosity was determined at the end of the measurement, which can be used as an indicator of processability.

3.3. Tensile and tear tests

We cut tensile and tear specimens from the hot-pressed sheets using a manual punching machine. The shape of the tensile specimens was in accordance with the type 5A dumbbell specimen of the ISO 527-2:2012 standard, and had a total length of 75 mm. The tear specimens conformed in shape to Die C of the ASTM 624-00 (2020) standard. Uniaxial tensile and tear tests were carried out at 25°C with a Z005 (Zwick Gmbh., Ulm, Germany) universal tensile tester using 20 kN-rated Zwick 8355 screw grips. The force was measured with a high-precision Zwick 5 kN load cell with a resolution of 0.01 N. In case of the tensile and tear tests, 5 and 3 displacement-controlled tests were performed with a 50 mm and a 56 mm gripping distance and a 500 mm/min crosshead speed, respectively. Strain was calculated based on the ratio of crosshead displacement and gripping distance.

3.4. Compression set tests

Compression set was measured in accordance with the ISO 815-1 standard with the use of Type B test specimens. The samples were exposed to a temperature of 70 °C for 24 hours. The initial thickness of the specimens was 6 mm, which decreased to 4.7 mm during the test, representing an approximately 22 % compression of the original thickness. After the compression period, the samples were allowed to recover at room temperature for 30 minutes before the recovered thickness was measured.

3.5. Hardness tests

The hardness of the samples was measured according to the ISO 48-4 Shore A method with a Zwick H04.3150.000 hardness tester (Zwick GmbH, Ulm, Germany). Indentation time was 3 s, and the load was 8.05 N.

3.6. Statistical analyses

Statistical analyses were conducted using Minitab 21.1.0 (Minitab LLC, State College, PA) and the Statistics and Machine Learning Toolbox of MATLAB R2022a (MathWorks, Natick, MA). The assumptions of normality and equal variance were tested using the Ryan–Joiner normality test and Levene's test, respectively. To examine the effect of biochar content on the vulcanization parameters (minimum torque, maximum torque, scorch time, and optimum curing time), a one-way analysis of variance (ANOVA) was performed, followed by a Tukey HSD (Honestly Significant Difference) post hoc test when necessary. The effect of biochar content on torque increase was examined using regression analysis. Regression analyses were also conducted to evaluate the effect of biochar content on the peak times and maximum values of the the time derivatives of the time-dependent storage modulus curves, as well as on the peak times of the loss factor curves. For the mechanical properties, regression analyses were applied to assess the influence of biochar content on tensile strength, modulus at 300 % strain, strain at break, and hardness. The effect of biochar content on tear strength was evaluated using the Mann–Whitney test, comparing BC0 with BC20, and low biochar content (≤20 %) with high biochar content (≥40 %). To examine the influence of biochar content on compression set, a Kruskal–Wallis test was performed, followed by Dunn's post hoc test. A significance level of α=0.05 was applied in all analyses. Details of the statistical procedures are provided in the supplementary material.

3.7. Evaluation of sustainability indicators

We present an estimate for the carbon dioxide (CO_2) footprint of the carbon black and the biochar fillers in the rubber mixtures. The estimates were calculated according to Eq. 1, where we considered the CO_2 emissions of the components based on literature data. Based on the IPCC Guidelines for National Greenhouse Gas Inventories, the production of 1 tonne of carbon black generates 5.25 tonnes of CO_2 [38]. In case of biochar production, direct emissions from pyrolysis typically range from ~90 to 200 kg carbon dioxide equivalent per tonne (CO_2eq/t) of biochar, depending on energy sources and process efficiency [39]. For example, the European Biochar Certificate (EBC) LCA reports ~87 kg CO_2eq/t for state-of-the-art pyrolysis systems using grid electricity and waste biomass [40]. Freres Lumber's environmental product declarations (EPD) for a biomass-fired pyrolysis system reports ~196 kg CO_2eq/t of biochar, largely from boiler combustion and on-site fuel [41]. When considering net cradle-to-gate greenhouse gas (GHG) balance, USDA's CharBoss reports a carbon-negative −2.7 tonnes CO_2eq/t of biochar, though direct process emissions are still consistent with other systems (likely under 200 kg CO_2eq/t) [42].

$$CO_2eq/t(fillers) = w_{CB}CF_{CB} + w_{BC}CF_{BC} \quad (1)$$

In this article, we present three estimates for CO_2 emission of biochar production using data from EBC [40], Freres [41] and CharBoss [42]. For carbon black, the same CO_2 emission was applied for all calculations with the use of data from IPCC Guidelines for National Greenhouse Gas Inventories.

Rubber manufacturing primarily consists of two energy-intensive stages: processing and curing, which together account for approximately two-thirds of the total energy consumption in the production process [43]. The processing stage includes the mixing of raw rubber compounds and preforming operations. The curing stage corresponds to the moulding process, during which vulcanization occurs. Post-vulcanization, finishing steps and additional unidentified consumptions were not considered. Based on the findings of Piccioni et al. [43], we examined two cases: the manufacture of tyres and tubes (Case 1), and the manufacture of other rubber products such as seals and hoses (Case 2). We calculated the energy demand for the NR composites with different BC contents presented in this article for both manufacturing routes.

The energy required for processing closely depends on the viscosity of the mixture, which can be characterized with the ML 1+4 Mooney viscosity. Mooney viscosity provides a measure of the compound's resistance to shear deformation under controlled temperature and rotational stress. Higher Mooney values indicate increased internal friction and decreased flowability, leading to greater energy input during mixing.

To quantify the energy demand of the curing process, we calculated the area under the vulcanization curve (S'(t)), corrected by subtracting the minimum torque (S'_{min}), over the time interval from t_{min} (the time when S'(t) reaches S'_{min}) to t_{90} (Eq. 2). This method ensures that only

the torque increase due to crosslinking is considered, excluding early effects like thermal softening that are not related to the actual vulcanization process. Subtracting S'_{min} sets the baseline for integration, allowing the calculated area to reflect the mechanical resistance developed during network formation, which is directly related to the energy needed for curing.

$$A_{vulc} = \int_{t_{min}}^{t_{90}} \left(S'(t) - S'_{min}\right) dt \quad (2)$$

To assess the impact of BC content on energy requirements, we calculated a normalized energy demand relative to the BC0 reference using Eq. 3. This equation considers both the processing and vulcanization stages, weighted according to their respective contributions to the overall energy consumption (w_1, w_2).

$$nED = w_1 \cdot \frac{ML\ 1+4_{BCx}}{ML\ 1+4_{BC0}} + w_2 \cdot \frac{A_{vulc,BCx}}{A_{vulc,BC0}} \quad (3)$$

where nED is the normalised energy demand, ML1+4 is the respective part of Mooney viscosity, w_1 and w_2 are weight fractions (where $w_1+w_2=1$), and the subscripts BC0 and BCx refer to the reference material without biochar and the materials with different biochar contents, respectively.

4. Results and discussion

4.1. Microstructure

Fig. 2 shows the raw rubber sheets collected from the two-roll mill before vulcanisation. The surface becomes progressively more matte with increasing BC content.

Fig. 3a shows scanning electron micrographs of the BC particles. The porous structure of the BC remains intact after grinding (Fig. 3b). We measured the characteristic (maximum) size of the particles (Fig. 3c) and then plotted the relative frequency histogram (Fig. 3d). Sieving was efficient, as particle sizes fell within the targeted range, with an average of 68.7±32 μm. Fig. 3e-i show the SEM-EDS results. Besides carbon, the chemical composition of the wood biochar consists of approximately 18 % oxygen, 1.6 % calcium, and smaller amounts of aluminium, silicium and potassium. The relative higher amount of oxygen indicates lower pyrolysis temperature [44].

Fig. 4 shows scanning electron microscopy images taken from the cross-section of each NR composite. We analysed cross-sections after tensile testing to gain insight into the damage mechanisms and the microstructure after deformation. The NR0 sample (Fig. 4a), which contains no biochar, exhibits a smooth fracture surface with visible CB aggregates ranging from 1 to 5 μm in size. The addition of BC significantly alters the fracture morphology, resulting in a rougher surface characterized by fragmented biochar particles and debris. The roughness refers to the increased energy distribution during crack propagation, as microcracks deflect around rigid BC particles and thus travel a longer distance. Up to 60 wt% BC content, CB particles remain occasionally visible. In some regions, larger BC particles (approximately 50 μm in size) are present, which have retained their porous structure despite processing and deformation (Fig. 4c). The presence of these larger particles can concentrate stress locally, which can initiate microcracks. Under load, the BC particles tend to fracture along their porous network and form a lamellar structure (Fig. 4e). This particle fracture contributes to filler–matrix debonding, as the newly created particle surfaces reduce the effective contact area with the rubber matrix and weaken stress transfer. Phase separation predominantly occurs at the biochar–rubber interfaces (Fig. 4d). However, in the case of larger BC particles with greater pore sizes, rubber infiltrates into the porous network (Fig. 4f). This infiltration can result in local mechanical interlocking, which delays complete pull-out.

4.2. Rheological and vulcanization characteristics

Fig. 5 shows the vulcanization curves measured with a rubber process analyser at 160°C. We took the curves to determine vulcanization time, and Table 4 presents the characteristic parameters calculated with the use of the curves. One-way ANOVA showed that there is no significant effect of biochar content, $F(5,12)=0.31$, $p=0.898$ on the minimum torque (S'_{min}). The maximum torque represents the stiffness of the fully cured rubber. Maximum torque increased by 20 % at 100 % BC compared to 0 % BC. One-way ANOVA showed significant group differences, $F(5,12)=17.79$, $p<0.001$, and Tukey's HSD confirmed the 0 % vs 100 % contrast as significant. The difference between the maximum and minimum torque increased with BC content, and this trend was significant, as comfired by linear regression ($F(1,16)=134.25$, $p<0.001$, $R^2=0.8869$). This might suggest that crosslink density also increases [45]. Regarding scorch time (t_{s2}), one-way ANOVA showed a significant effect of BC content ($F(5, 12)=3.71$, $p=0.029$). However, Tukey's HSD indicated that only the BC100 type samples differed from BC20 and BC40; no other significant difference was found. Therefore, we can conclude that scorch time shows no consistent change as a function of BC content. Optimum curing time (t_{90}) did not differ across biochar contents (one-way ANOVA: $F(5,12)=0.90$, $p=0.511$). Overall, it can be concluded that BC does not significantly alter the vulcanization characteristics, even at 100 % BC content. This indicates that BC shows potential as a more sustainable and cost-effective partial replacement to carbon black.

Fig. 6a shows that the storage modulus (G') generally increases with increasing BC content. Between 400 s and 600 s, the storage modulus reaches a plateau, with values of G'=761±26 kPa and G'=916±27 kPa for NR0 and NR100, respectively. At 20 % biochar content, the storage modulus decreases to G'=804±21 kPa. Fig. 6b shows the time derivatives of the G'(t) curves. Both the increasing peak times of the dG′/dt curves (regression analysis: $R^2=0.53$, $F(1,16)=20.46$, $p<0.001$) and the corresponding shift in the peak of tan δ(t) (Fig. 6d) (regression analysis: $R^2=0.50$, $F(1,16)=17.77$, $p<0.001$) indicate a delayed onset of network formation, although the moderate correlations suggest that these effects are not particularly strong. Similarly, Abidin et al. [34] also found that increasing BC content reduces cure time and enhances cure rate in the case of nitrile butadiene rubbers. The increase in the maximum value of the dG′/dt peaks indicates that, once initiated, the crosslinking process

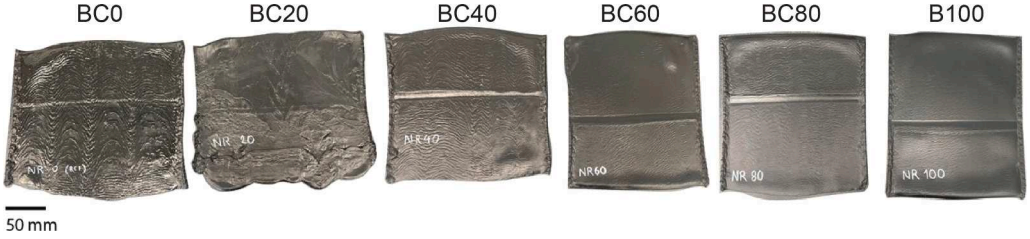

Fig. 2.. Natural rubber (NR) composites with different biochar (BC) contents collected from the two-roll mill. (Label "BC" refers to biochar, and the number indicates the BC content as a substitute to carbon black (CB)).

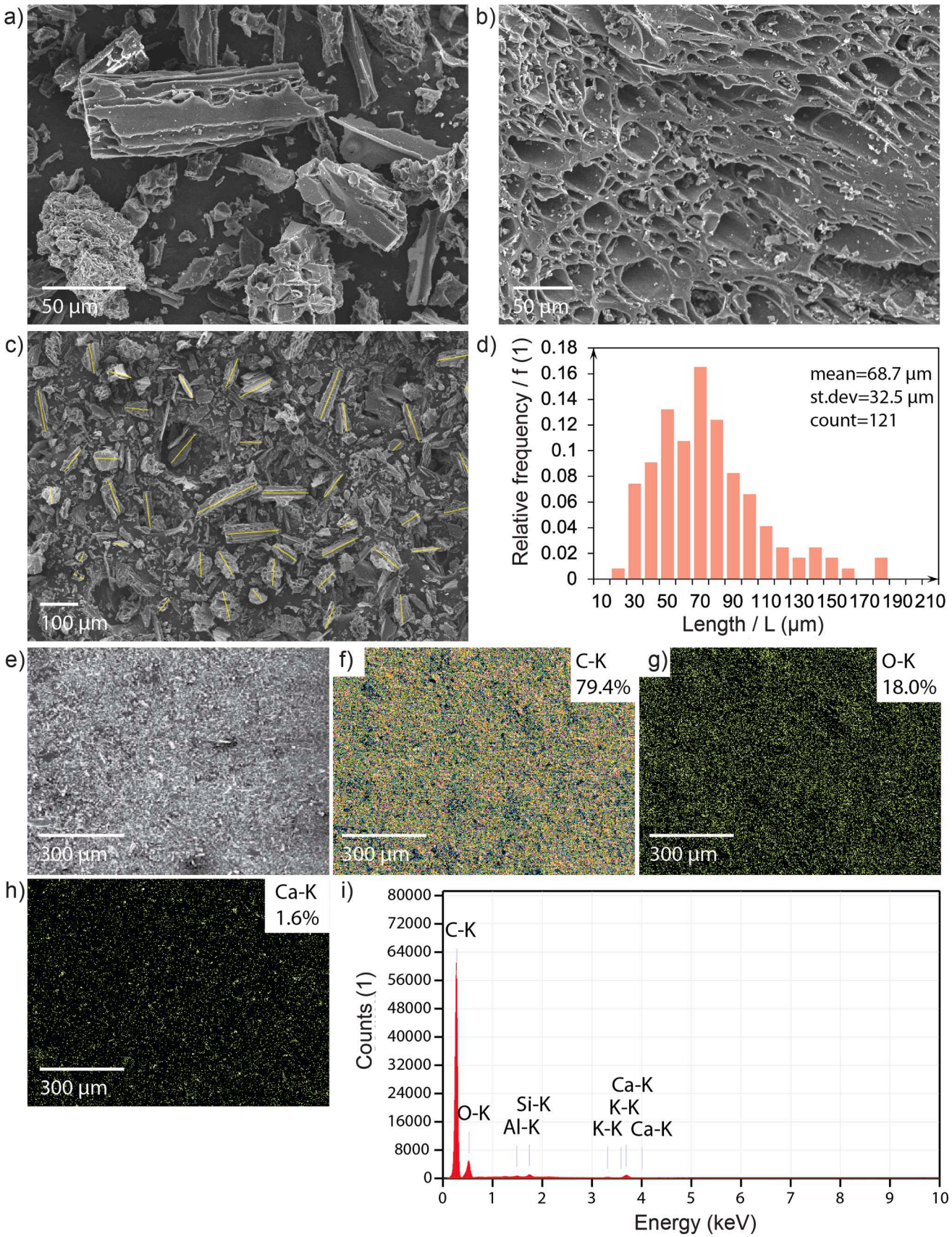

Fig. 3.. Microstructure and size distribution of the biochar particles used as filler in the NR composites: a) biochar particles; b) porous structure of a single biochar; c) measurement of the maximum lengths; d) size distribution; Scanning Electron Microscope - Energy Dispersive Spectroscopy (SEM-EDS) results: e) micrograph of the sampling area; elemental maps: f) C-K, g) O-K, h) Ca-K; i) EDS spectrum.

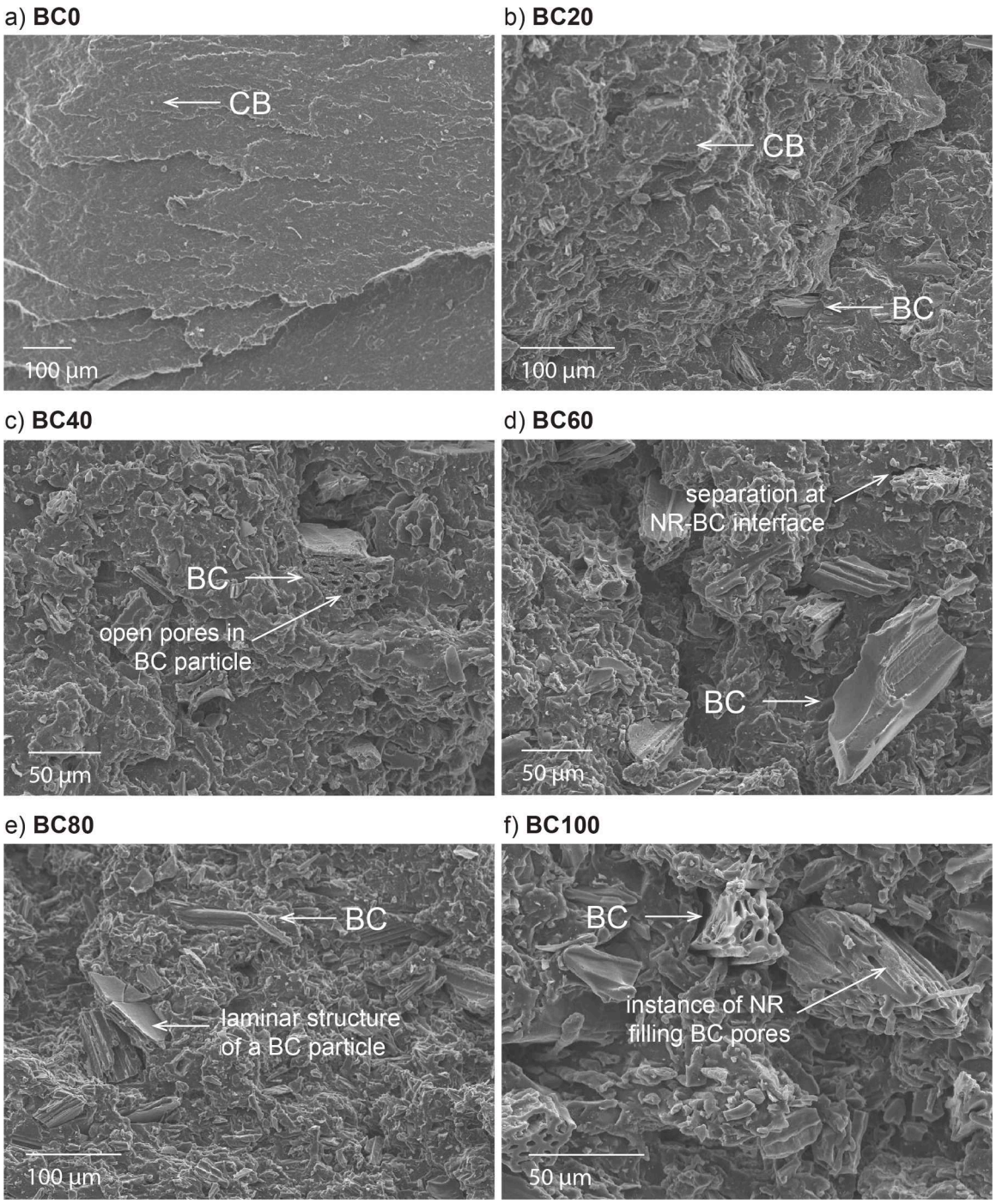

Fig. 4. Microstructure of the fracture surfaces after tensile testing in the case of the a) BC0, b) BC20, c) BC40, d) BC60, e) BC80, f) BC100. ("BC" refers to biochar, and the number indicates BC content as a substitute to carbon black (CB)).

proceeds at a faster rate, which is supported by a strong and statistically significant correlation (regression analysis: R^2=0.83, $F(1,16)$=83.62, p<0.001). In summary, these observations suggest that biochar delays the onset of crosslinking but subsequently accelerates the reaction rate. Fig. 6c shows that as biochar content increases, the loss modulus G″ also increases, indicating more energy dissipation during dynamic deformation. This increase likely results from higher internal friction.

Fig. 7a shows the Mooney viscosity curves measured at 100 °C. The curves exhibit similar profiles for all formulations, characterized by an initially high viscosity followed by a gradual decreasing trend throughout the measurement period. Fig. 7b shows that the ML 1+4 Mooney viscosity increases with increasing biochar content. This suggests that processing becomes more energy-intensive with increasing biochar content, due to greater stiffness and internal resistance to flow in the unvulcanised state. Biochar particles, used as fillers, are inherently rigid and porous, and their particle size is typically an order of magnitude larger than that of carbon black. This larger size, combined with their morphology, restricts polymer chain mobility and contributes to the increased viscosity of the compound.

4.3. Mechanical properties

We characterized the mechanical performance of the NR composites by their tensile properties (tensile strength, strain at break, and

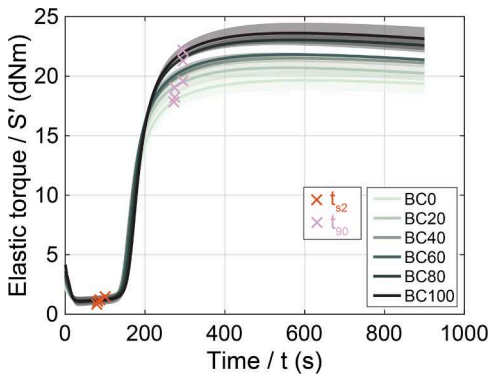

Fig. 5. Vulcanization curves at 160°C for NR composites containing 0-100 % biochar. Scorch time (t_{s2}) and optimum cure time (t_{90}) are indicated. ("BC" refers to biochar, and the number indicates BC content as a substitute to carbon black (CB)).

Table 4
Vulcanization characteristics of natural rubber (NR) composites containing 0-100 % biochar (BC) at 160°C. ("BC" refers to biochar, and the number indicates BC content as a substitute to carbon black (CB)).

Biochar content (%)	Minimum torque S'_{min} (dNm)	Maximum torque S'_{max} (dNm)	Torque increase S'_{min}-S'_{max} (dNm)	Scorch time at 160°C (t_{s2}) (s)	Optimum cure time at 160°C (t_{90}) (s)
0	1.27±0.05	19.7±0.8	18.4±0.9	146±7	268±11
20	1.16±0.08	20.7±0.6	19.5±0.7	144±3	258±5
40	1.16±0.15	21.5±0.3	20.4±0.4	145±2	262±4
60	1.06±0.21	21.8±0.1	20.8±0.3	146±2	261±11
80	1.11±0.34	23.1±0.5	21.9±0.1	151±3	267±11
100	1.07±0.40	23.6±0.9	22.6±0.5	156±4	271±9

modulus), tear strength, and Shore A hardness. Fig. 8a shows the stress–strain curves of the NR formulations. The curves change in a trend-like manner with increasing BC content. Tensile strength, strain at break and modulus at 300 % strain decrease as a function of BC content. However, at low strains (ε<100 %), the initial section of the curve changes from convex to concave (Fig. 8b), i.e. at small strains, biochar increases stiffness. This is consistent with the findings for the plateau phase of the time-dependent storage modulus (G'(t)) curves determined with the rubber process analyser (see Section 4.2.). This increased stiffness at low strains may be advantageous in applications requiring dimensional stability, vibration damping, or structural support under small deformations.

Fig. 8c shows the tensile strength, strain at break and modulus at 300 % strain of the rubber composites as a function of BC content. Linear regression confirmed strong linear trends: tensile strength (R^2=0.9664, F(1,28)=835.46, p<0.001), modulus at 300 % strain (R^2=0.9606, F(1,28)=708.18, p<0.001), and a moderate trend for strain at break (R^2=0.6907, F(1,28)=65.75, p<0.001). This means that tensile strength and modulus are reliably predictable depending on the BC content. NR composites with 0 % BC content had the highest tensile values, indicating that the addition of biochar gradually deteriorates the properties of the composites. Overall, the increase in initial stiffness followed by a decrease in tensile strength and strain at break shows that BC acts as reinforcement in the case of small deformations. However, in the case of larger deformations, the porous structure of BC particles causes defects that accelerate crack propagation and lead to premature failure.

The slight, linearly decreasing trend is similar to the effects observed in the literature, but there are differences in the rate of decrease. Peterson and Chisholm [25], found an initial increase in tensile strength at 10 % BC content, which can be attributed to the beneficial effects of pistachio shell feedstock. Chueangchayaphan et al. [46] reported a decrease in tensile strength and elongation, but they found a more than 100 % increase in modulus at 300 % strain. The authors used oil palm trunk biochar. These differences confirm that the mechanical performance of NR composites greatly depends on biochar properties.

Fig. 8d shows tear strength as a function of BC content. Tear strength determines the resistance of a material to the growth of cuts or cracks under load. This is a critical property in applications where rubber is exposed to sharp objects, or cyclic loads. With increasing BC content, mean tear strength decreased from 32.1 MPa at 0 % BC to 9.5 MPa at 100 % BC. Tear strength did not differ between 0 % and 20 % BC (Mann–Whitney test: W=13, p=0.383), whereas the low-BC group (0–20 %) was significantly higher than the high-BC group (40–100 %) (Mann–Whitney test: W =93, p=0.001), indicating that the substantial decrease occurs beyond 20 % BC. A decrease in tear strength with increasing BC content may be attributed to poor interfacial adhesion between the BC and the NR matrix. Debonding at the NR-BC interface can be seen in the SEM images (see Section 4.1.). In addition, the porous structure of biochar can also influence this property. However, Chueangchayaphan et al. [46] reported a slight increase in tear strength when using oil palm trunk biochar. Since tear strength is a result of the failure process, it is greatly influenced by the compatibility and interface properties between the filler and the matrix.

In the case of Shore A hardness, there is a linear increase with higher BC contents (F(1,28)=60.38, p<0.001, R^2=0.672) (Fig. 8e). This is primarily due to the stiffening effect of the filler. As BC content increases, the rubber matrix becomes denser with rigid particles, which limits the mobility of polymer chains and reduces surface deformability. Miedzianowska-Masłowska et al. [32] also found an increase in Shore A hardness with increasing BC content with BC produced from beech wood.

For compression set, Kruskal–Wallis test showed overall differences (H(5)=13.65, p=0.018), but posthoc Dunn's test found only one significant pair (40 % vs 100 %), with all others non-significant. Therefore, no consistent or practically meaningful trend with BC content was evident. This suggests that BC content does not influence long-term elastic recovery, and the permanent deformation behaviour of the composite is primarily governed by the characteristics of the NR matrix.

4.4. Evaluation of mechanical performance and sustainability

We estimated the CO2 footprint of the carbon black and biochar fillers used in the rubber mixtures, taking into account the CO_2 emissions of each component based on literature data. Fig. 9 shows the results: even with a 20 % replacement of carbon black with biochar, the CO_2 emission from fillers is reduced by 19–30 % depending on biochar production. According to different approaches, biochar can be considered CO_2 neutral or CO_2 negative. Using a CO_2 negative estimate (CharBoss) the emissions from carbon black are completely offset by the biochar above 60 % content.

We also quantified the energy demand of the curing process using the method described in Chapter 3.7. The results are summarized in Table 5. Case 1 refers to the processing and curing of tyres and tubes while Case 2 refers to other rubber products such as seals and hoses. In both cases, the normalised energy demand increases with increasing biochar content. This is in line with the linear increase in Mooney viscosity. As the biochar content increases, viscosity increases, which requires greater mixing power and thus leads to greater energy consumption.

Fig. 10 presents a comprehensive evaluation of the NR composites with different BC contents, incorporating both mechanical performance and sustainability indicators. Table 6 presents a comparison of the results of this paper with those of others from the literature. Previous studies differ greatly in terms of biochar feedstock and filler size; therefore, the mechanical performance of the rubber compounds also varies. Generally, a slight increase in minimum torque can be noted with higher biochar ratios, which suggests an increase in viscosity. Among the studies examined, the largest biochar filler size was applied in this

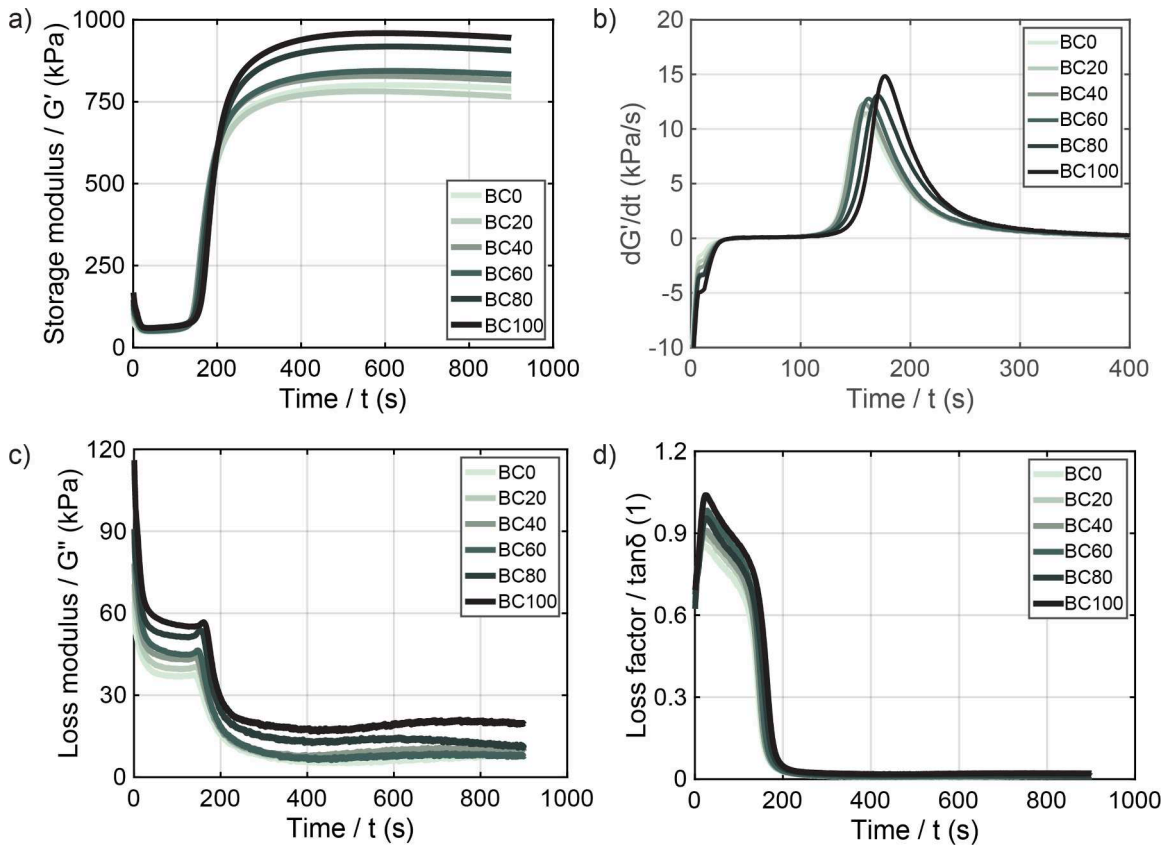

Fig. 6. Time-dependent, dynamic rheological properties of the NR composites containing 0-100 % biochar at 160°C (showing one characteristic curve for each): a) storage modulus, b) time derivative of the storage modulus, c) loss modulus, d) loss factor. ("BC" refers to biochar, and the number indicates BC content as a substitute to carbon black (CB)).

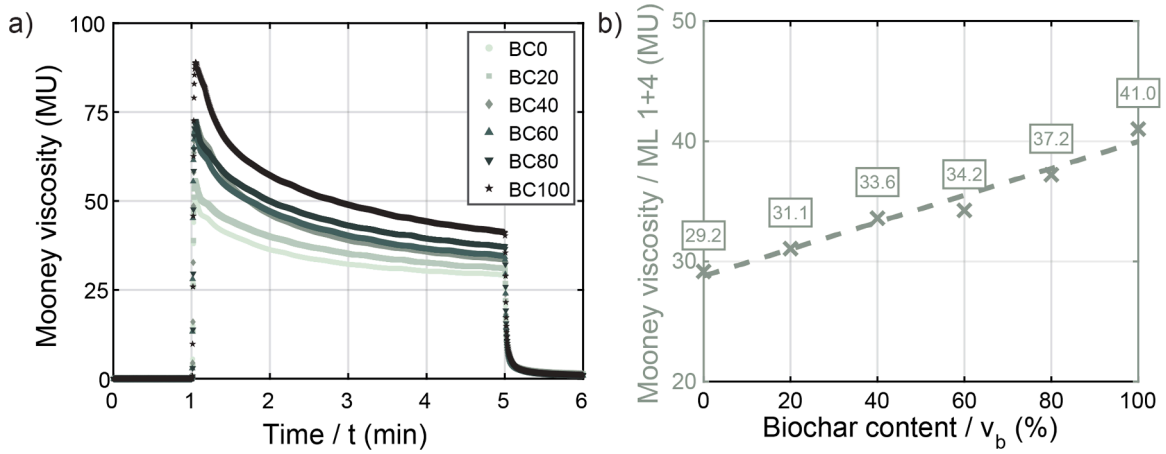

Fig. 7. Mooney viscosity of the NR compounds: a) time-dependent Mooney viscosity curves measured at 100 °C, and b) the ML 1+4 Mooney viscosity values as a function of biochar content. ("BC" refers to biochar, and the number indicates BC content as a substitute to carbon black (CB)).

research. This may explain the decrease in tensile properties. At the same time, achieving a smaller particle size is a time-consuming and energy-intensive process; in several cases, multi-stage grinding was used, and only on a laboratory scale. None of the studies listed examined sustainability indicators. In our research, sustainability was assessed with the use of the calculated CO_2 emissions (kgeq/t) of the fillers and the normalized energy demand (%) associated with rubber production. In both cases, the most conservative (i.e., least favourable) values were applied. Mechanical performance was characterized by tensile strength (MPa), elongation at break (%), modulus at 300 % strain (MPa), and tear strength (kN/m). There is a clear trade-off between sustainability and mechanical performance in NR composites reinforced with varying amounts of BC. As BC content increases, the environmental impact significantly decreases, but this is accompanied by a gradual decline in mechanical properties. Our results show that the most promising BC content is 20 %, where mechanical properties deteriorated by a maximum of 15 % (modulus at 300 % strain). At the same time, the CO_2 footprint is reduced by 20 %, and the energy demand of production remained at its lowest level.

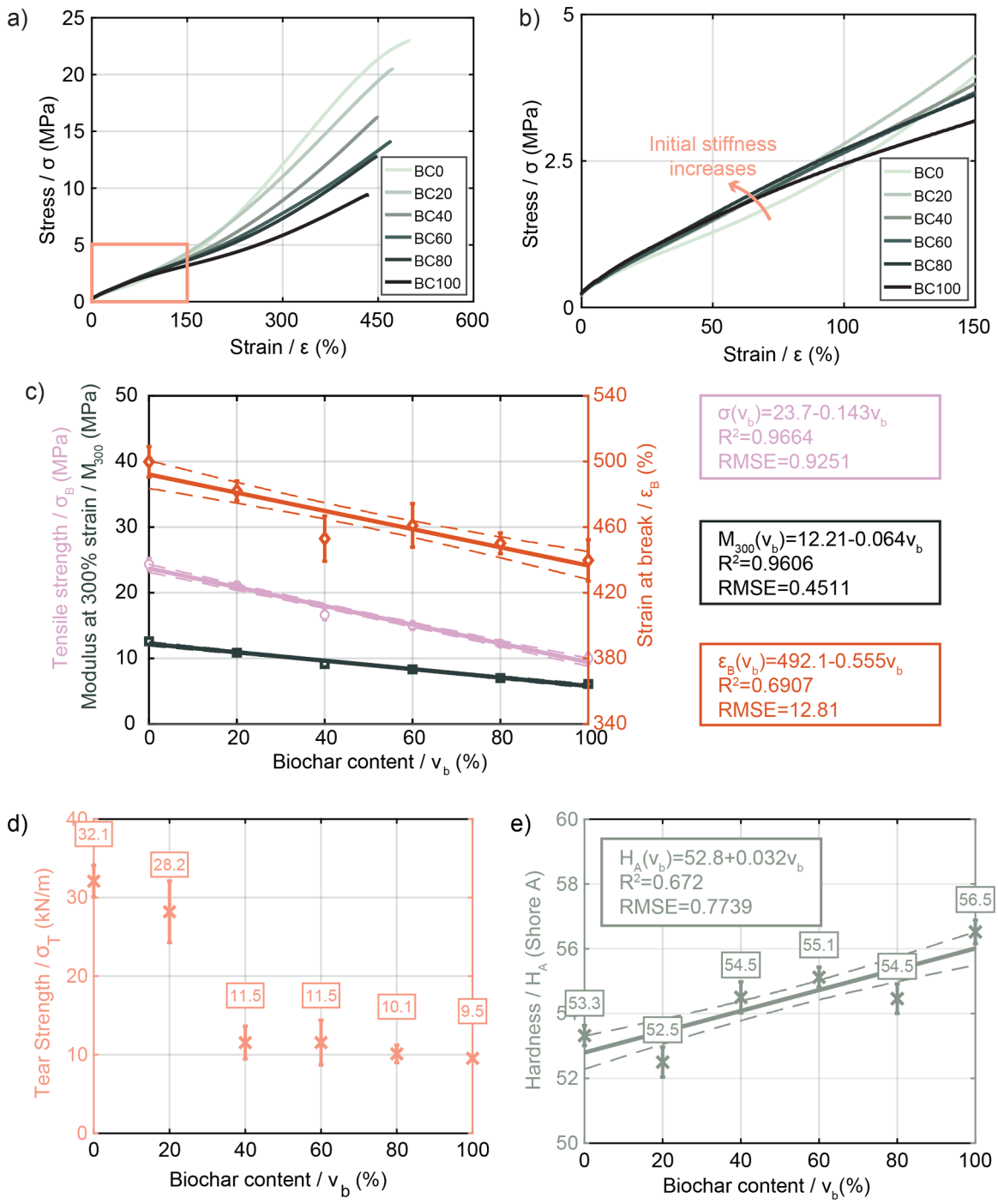

Fig. 8. Mechanical test results for the natural rubber (NR) composites with different biochar (BC) contents: a) stress–strain curves, b) stress–strain curves showing increase in initial stiffness; c) linear trends for tensile strength, modulus at 300 % strain and strain at break; d) tear strength and e) linear trend in Shore A hardness. ("BC" refers to biochar and the number indicates BC content as a replacement of carbon black (CB)). The thin dashed lines indicate the 95 % confidence intervals.

4.5. Limitations

One limitation to generalizing the current results is the variability in biochar filler. The type of feedstock and production conditions significantly influence the chemical composition, surface characteristics, and consequently the performance of biochar in rubber composites [14]. For example, Li et al. [47] show that for wood biochars, high pyrolysis temperature (>500°C) increased carbon content and pore volume compared to low pyrolysis temperature (≤500°C). Chowdhury et al. [48] also found that besides carbon content, increasing pyrolysis temperature also increases the Brunauer-Emmett-Teller (BET) surface area in the case of durian wood sawdust.

The CO_2 and energy demand calculations presented in our study are not based on a life cycle assessment (LCA), but on estimates derived from the literature. No standardized LCA framework was used. Energy demand analysis relies on indirect indicators (Mooney viscosity and vulcanization curves), which only provide an approximate measure of processing efficiency and cannot fully represent industrial-scale energy consumption. These methodological simplifications result in uncertainty.

The CO_2 emission of biochar production can vary significantly depending on the type of feedstock, pyrolysis conditions, and system

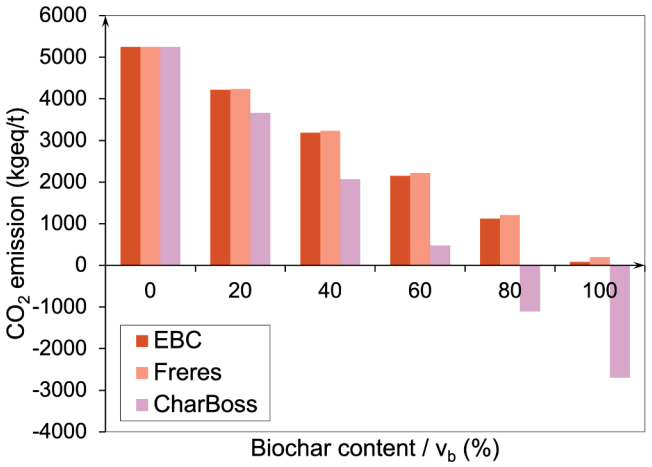

Fig. 9. Carbon dioxide (CO_2) footprint of the natural rubber (NR) composites with different biochar (BC) content. BC content should be interpreted as a substitute to carbon black (CB).

Table 5
Normalised energy demand for the natural rubber (NR) composites with different biochar (BC) contents. Biochar content should be interpreted as a substitute to carbon black.

Biochar content (%)	Area under curve A_{vulc} (dNm·s)	Case 1 Normalised energy demand nED (1) (w_1=0.2, w_2=0.8)	Case 2 Normalised energy demand nED (1) (w_1=0.7, w_2=0.3)
0	1500±127	1.00	1.00
20	1473±36	0.92	1.01
40	1589±64	1.00	1.10
60	1580±105	1.07	1.13
80	1669±133	1.15	1.23
100	1700±110	1.17	1.32

boundaries. Using Monte Carlo simulations, Kane et al. [17] shows that in a "best-practice" scenario (high energy efficiency, short transport, energy recovery), biochar production yields a net carbon removal of 1.4 kg CO_2e per kg biomass; whereas in a "poor practice" scenario (low efficiency, long transport, no energy recovery), the median result was net emission of 0.090 kg CO_2e per kg biomass. At the same time, higher pyrolysis temperatures generally result in biochars with better mechanical and structural properties, such as higher carbon content and surface area. However, these conditions increase energy requirements and thus also potential CO_2 emissions. Optimizing biochar production therefore requires a careful balance between sustainability and performance, where the environmental footprint of the process must be weighed against the desired material properties. From an economic point of view, biochar can be a cost-competitive alternative to carbon black, especially when produced from low-cost or waste wood feedstocks. Reported production costs for biochar typically range from 0.2 to 1.5 USD/kg, while carbon black generally costs around 2 USD/kg or higher, depending on grade and application [49,50]. The overall cost balance depends on feedstock availability, process efficiency, and scale. Biochar also offers an additional economic advantage through potential carbon credit revenues.

5. Conclusion

In the pursuit of sustainable alternatives to carbon black (CB), biochar (BC) has emerged as a promising renewable alternative in natural rubber (NR) composites. In this study, we investigated the feasibility of replacing CB with wood-derived BC in NR composites as a substitution of CB at varying filler contents (0 %, 20 %, 40 %, 60 %, 80 %, and 100 % replacement levels). The results showed that BC enhances stiffness at low strains, which may be advantageous in applications with small deformations. However, under larger strains, the porous morphology of BC leads to crack propagation, reducing tensile strength and elongation at break. Overall, with increasing BC content, tensile strength, strain at break, and modulus at 300 % strain declined linearly. Strong linear correlations have been identified and statistically proven, which contribute to the predictability of the mechanical properties of biochar-based rubber compounds. Meanwhile, Mooney viscosity tests revealed that with increasing BC content, the resistance to flow in the unvulcanised state also increases, suggesting that processing becomes more energy-intensive. Additionally, BC delayed the onset of vulcanization but subsequently accelerated the cure reaction rate. The environmental impact was evaluated through estimates of CO_2 emissions and normalized energy demand—an approach not previously reported for wood biochar–based rubber composites. Our analysis showed that a BC content of 20 % was favorable, at which mechanical properties deteriorated by no more than 15 %, while the CO_2 footprint of the composite was reduced by 20 % and energy requirements remained at the lowest level. Such a composition could be suitable for applications such as seals,

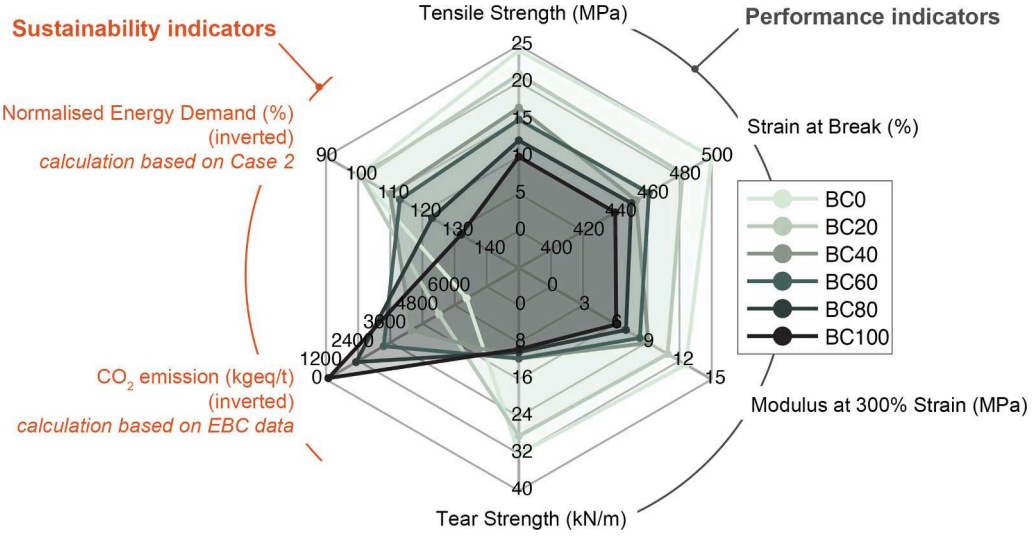

Fig. 10. Overview of the mechanical performance and sustainability indicators of natural rubber (NR) composites with different biochar (BC) contents. ("BC" refers to biochar and the number indicates BC content as a substitute to carbon black (CB)).

Table 6
Comparison of biochar-filled rubbers in terms of filler type, main mechanical and processing properties. The percentage change is interpreted relative to BC0 mixtures, with the largest decrease (min) and the largest increase (max) indicated.

Biochar source	Substitution ratio (phr)	Particle size	Change in tensile strength (min-max)	Change in elongation at break (min-max)	Minimum torque (dNm)	Sustainability indicators	Source
Pistachio shell	0, 10, 20, 30, 40, 50	2 μm (mean)	+10 % (10 phr), -8 % (50 phr)	+20 % (10 phr), +22 % (40 phr)	-	Not investigated	[25]
Oat straw	0, 10, 20, 30	<45 μm	+88 % (10 phr), +218 % (20 phr)	-22 % (30 phr), +5 % (10 phr)	0.58 (0 phr) – 0.25 (30 phr)	Not investigated	[27]
Bamboo waste	0, 10, 20	17 μm (mean)	+240 % (10 phr), +248 % (20 phr)	+69 % (10 phr), +59 % (20 phr)	-	Not investigated	[31]
Beech wood	0, 10, 20, 30	-	+80 % (10 phr), +45 % (30 phr)	-13 % (10 phr), -25 % (30 phr)	0.4 (0 phr) – 0.42 (30 phr)	Not investigated	[32]
Palm kernel shell	0, 5, 10, 15, 20, 25, 30, 35	53 μm	-	-	2.13 (0 phr) – 3.04 (35 phr)	Not investigated	[34]
Nut shell and grain husk	55	-	+22 % −32 %	+34 %, −16 %	-	Not investigated	[35]
Hardwood waste	0, 10, 20, 30, 40	0.5-3 μm	-	-	2.96 (0 phr) – 3.86 (10 phr)	Not investigated	[36]
Wood waste	0, 10, 20, 30, 40, 50	≤75 μm	-13 % (10 phr) -59 % (50 phr)	-3.6 % (10 phr) -12 % (50 phr)	1.16 (10 phr)	- Normalised energy demand - CO_2 emission	current study

vibration-damping elements, and other non-structural rubber products where moderate mechanical performance is acceptable. Overall, our study shows that when used in suitable amounts, BC offers a viable pathway towards more sustainable rubber products.

CRediT authorship contribution statement

Ábris Dávid Virág: Writing – original draft, Visualization, Validation, Methodology, Investigation, Formal analysis, Conceptualization. **Ákos Görbe:** Writing – original draft, Methodology, Investigation. **Andrea Kohári:** Writing – original draft, Methodology, Investigation. **Csenge Tóth:** Writing – review & editing, Visualization, Supervision, Project administration, Methodology, Conceptualization.

Declaration of competing interest

The authors declare that they have no known competing financial interests or personal relationships that could have appeared to influence the work reported in this paper.

Acknowledgements

Project no. TKP-6-6/PALY-2021 has been implemented with the support provided by the Ministry of Culture and Innovation of Hungary from the National Research, Development and Innovation Fund, financed under the TKP2021-NVA funding scheme. This work was supported by the National Research, Development and Innovation Office (K146085). Ábris Dávid Virág is thankful for the support of the EKÖP-25-4-II-BME-212 University Research Fellowship Programme of the Ministry for Culture and Innovation from the source of the National Research, Development, and Innovation Fund. Csenge Tóth is thankful for the support of the EKÖP-25-4-II-BME-214 University Research Fellowship Programme of the Ministry for Culture and Innovation from the source of the National Research, Development, and Innovation Fund.

Supplementary materials

Supplementary material associated with this article can be found, in the online version, at doi:10.1016/j.rineng.2025.107843.

Data availability

Data will be made available on request.

References

[1] Y. Fan, G.D. Fowler, M. Zhao, The past, present and future of carbon black as a rubber reinforcing filler – A review, J. Clean. Prod. 247 (2020) 119115, https://doi.org/10.1016/J.JCLEPRO.2019.119115.
[2] K. Meisel, L. Röver, S. Majer, B. Herklotz, D. Thrän, A comparison of functional fillers—Greenhouse gas emissions and air pollutants from lignin-based filler, carbon black and silica, Sustainability 14 (2022), https://doi.org/10.3390/su14095393.
[3] A. Chelli, H. Mechakra, A. Chellil, D.E. Tria, W. Bessa, K. Ikkache, B. Safi, Evaluation of viscoelastic performance and molecular structures of natural rubber/NBR blends reinforced by carbon black and nano-silica, Period. Polytech. Mech. Eng. 68 (2024) 162–171, https://doi.org/10.3311/PPme.28792.
[4] V.F. Lotfy, A.H. Basta, E.S. Shafik, Assessment the performance of chemical constituents of agro wastes in production safety alternative carbon black filler in rubber composite purpose, Sci. Rep. 15 (2025) 11035, https://doi.org/10.1038/s41598-025-92404-y.
[5] M. Džuganová, R. Stoček, M. Pöschl, J. Kruželák, A. Kvasničáková, J. Hronkovič, J. Preťo, Strategy for reducing rubber wear emissions: the prospect of using calcium lignosulfonate, Express Polym. Lett. 18 (2024) 1277–1290, https://doi.org/10.3144/expresspolymlett.2024.95.
[6] S.T. Kumbalaparambil, A.H. Chandaparambil, K. Naskar, Sustainable ZnO nanoparticles using sweet lime peel extract: eco-friendly activator in rubber for tire applications, Express Polym. Lett. 18 (2024) 991–1007, https://doi.org/10.3144/expresspolymlett.2024.76.
[7] F. Rosner, T. Bhagde, D.S. Slaughter, V. Zorba, J. Stokes-Draut, Techno-economic and carbon dioxide emission assessment of carbon black production, J. Clean. Prod. 436 (2024) 140224, https://doi.org/10.1016/J.JCLEPRO.2023.140224.
[8] S. Wu, Z. Wang, S. Guo, Y. Cai, J. Zhang, C. Huangfu, Y. Huang, L. Ma, W. Zhao, Life-cycle-based reconfiguration of sustainable carbon black production: integrated conventional technique with waste tire pyrolysis and its future improvement potentials, J. Clean. Prod. 442 (2024) 141022, https://doi.org/10.1016/J.JCLEPRO.2024.141022.
[9] A.N. Uttaravalli, S. Dinda, V.R. Kakara, A.V.R. Rao, T. Daida, B.R. Gidla, Sustainable use of recycled soot (carbon black) for the cleaner production of value-added products: A compendium, Chem. Eng. J. Adv. 11 (2022) 100324, https://doi.org/10.1016/J.CEJA.2022.100324.
[10] M. Sagar, K. Nibedita, N. Manohar, K.R. Kumar, S. Suchismita, A. Pradnyesh, A. B. Reddy, E.R. Sadiku, U.N. Gupta, P. Lachit, J. Jayaramudu, A potential utilization of end-of-life tyres as recycled carbon black in EPDM rubber, Waste Manage. 74 (2018) 110–122, https://doi.org/10.1016/J.WASMAN.2018.01.003.
[11] C. Dwivedi, S. Manjare, S.K. Rajan, Recycling of waste tire by pyrolysis to recover carbon black: alternative & environment-friendly reinforcing filler for natural rubber compounds, Compos B Eng. 200 (2020) 108346, https://doi.org/10.1016/J.COMPOSITESB.2020.108346.

[12] W.B.Setianto Nasruddin, P.Atmaji Lanjar, S. Agustini, E.P.Wulandari Rienoviar, T. I. Sari, B. Ibrahim, Utilization of spent bleaching earth as green filler and plasticizer in the manufacture of rubber compounds for solid tire production, Res. Eng. 23 (2024) 102690, https://doi.org/10.1016/J.RINENG.2024.102690.
[13] L. Karunanayake, T. Etampawala, D.J. de Silva, J. Bandara, A.U. Rajapaksha, M. Vithanage, Role and potential of biochar as a sustainable alternative reinforcing filler to carbon black in rubber composites, Biochar 7 (2025) 60, https://doi.org/10.1007/s42773-025-00429-3.
[14] S. Greenough, M.J. Dumont, S. Prasher, The physicochemical properties of biochar and its applicability as a filler in rubber composites: A review, Mater. Today Commun. 29 (2021) 102912, https://doi.org/10.1016/J.MTCOMM.2021.102912.
[15] Y. Zhang, M. He, L. Wang, J. Yan, B. Ma, X. Zhu, Y.S. Ok, V. Mechtcherine, D.C. W. Tsang, Biochar as construction materials for achieving carbon neutrality, Biochar. 4 (2022) 59, https://doi.org/10.1007/s42773-022-00182-x.
[16] R.S. Raj, S. Jain, Assessment of municipal solid waste torrefaction for sustainable biochar production: A comprehensive life cycle evaluation of eight process scenarios, Res. Eng. 27 (2025) 107025, https://doi.org/10.1016/J.RINENG.2025.107025.
[17] S. Kane, A. Bin Thaneya, A.P. Gursel, J. Fan, B. Bose, T.P. Hendrickson, S. L. Nordahl, C.D. Scown, S.A. Miller, A. Horvath, Uncertainty in determining carbon dioxide removal potential of biochar, Environ. Res. Lett. 20 (2024) 14062, https://doi.org/10.1088/1748-9326/ad99e9.
[18] Q. Zhang, W. Yi, Z. Li, L. Wang, H. Cai, Mechanical properties of Rice husk biochar reinforced high density polyethylene composites, Polymers (Basel) 10 (2018), https://doi.org/10.3390/polym10030286.
[19] D.Singh Karam, P. Nagabovanalli, K. Sundara Rajoo, C.Fauziah Ishak, A. Abdu, Z. Rosli, F. Melissa Muharam, D. Zulperi, An overview on the preparation of rice husk biochar, factors affecting its properties, and its agriculture application, J. Saudi Society of Agricult. Sci. 21 (2022) 149–159, https://doi.org/10.1016/J.JSSAS.2021.07.005.
[20] P. Hoang, Z. Zhang, J. Ren, Y. Peng, J. Cao, Versatile biochar for wood-plastic composites: improving mechanical properties, dimensional and thermal stability, Polym. Compos. 45 (2024) 10349–10364, https://doi.org/10.1002/pc.28477.
[21] Y. Wang, Y. Hu, X. Zhao, S. Wang, G. Xing, Comparisons of biochar properties from wood material and crop residues at different temperatures and residence times, Energy Fuels 27 (2013) 5890–5899, https://doi.org/10.1021/ef400972z.
[22] E.N. Yargicoglu, B.Y. Sadasivam, K.R. Reddy, K. Spokas, Physical and chemical characterization of waste wood derived biochars, Waste Manage. 36 (2015) 256–268, https://doi.org/10.1016/J.WASMAN.2014.10.029.
[23] A. Tomczyk, Z. Sokołowska, P. Boguta, Biochar physicochemical properties: pyrolysis temperature and feedstock kind effects, Rev. Environ. Sci. Biotechnol. 19 (2020) 191–215, https://doi.org/10.1007/s11157-020-09523-3.
[24] J.M. Jung, J.I. Oh, K. Baek, J. Lee, E.E. Kwon, Biodiesel production from waste cooking oil using biochar derived from chicken manure as a porous media and catalyst, Energy Convers. Manag. 165 (2018) 628–633, https://doi.org/10.1016/J.ENCONMAN.2018.03.096.
[25] S.C. Peterson, B.J. Chisholm, Utilizing Pistachio Shell Biochar to replace carbon black in natural rubber composites, J. Compos. Sci. 8 (2024), https://doi.org/10.3390/jcs8110482.
[26] C. Jiang, J. Bo, X. Xiao, S. Zhang, Z. Wang, G. Yan, Y. Wu, C. Wong, H. He, Converting waste lignin into nano-biochar as a renewable substitute of carbon black for reinforcing styrene-butadiene rubber, Waste Manage. 102 (2020) 732–742, https://doi.org/10.1016/J.WASMAN.2019.11.019.
[27] J. Miedzianowska-Masłowska, M. Masłowski, M. Delekta, K. Strzelec, Waste management of straw to manufacture biochar: an alternative reinforcing filler for natural rubber biocomposites, Ind. Crops Prod. 222 (2024) 119629, https://doi.org/10.1016/J.INDCROP.2024.119629.
[28] N. Bélanger, H. Macek, Y. Gariépy, M. Francis, S. Prasher, C.Y. Khripin, J. J. Mehlem, M.J. Dumont, Evaluating corn-based biochar as an alternative to carbon black in styrene-butadiene rubber composites, Mater Today Commun. 34 (2023) 105218, https://doi.org/10.1016/J.MTCOMM.2022.105218.
[29] I. Sittitanadol, N.L. Srakeaw, P. Somdee, P. Chumsamrong, S. Noyming, W. Singsang, N. Prasoetsopha, Utilizing coconut biochar as a bio-reinforcing agent in natural rubber composites, Starch - Stärke 77 (2025) 2400168, https://doi.org/10.1002/star.202400168.
[30] J. Lubura, P. Kojić, B. Ikonić, J. Pavličević, D. Govedarica, O. Bera, Influence of biochar and carbon black on natural rubber mixture properties, Polym. Int. 71 (2022) 1347–1353, https://doi.org/10.1002/pi.6439.
[31] J.Mago Sunali, A. Negi, K.K. Pant, S. Fatima, Development of natural rubber-bamboo biochar composites for vibration and noise control applications, J Clean. Prod. 373 (2022) 133760, https://doi.org/10.1016/J.JCLEPRO.2022.133760.
[32] J. Miedzianowska-Masłowska, M. Masłowski, K. Strzelec, Biomass, Phyto-ash, and biochar from beech wood as functional additives for natural rubber-based elastomer composites, Materials (Basel) 18 (2025), https://doi.org/10.3390/ma18071659.
[33] C. Jiang, J. Bo, X. Xiao, S. Zhang, Z. Wang, G. Yan, Y. Wu, C. Wong, H. He, Converting waste lignin into nano-biochar as a renewable substitute of carbon black for reinforcing styrene-butadiene rubber, Waste Manage. 102 (2020) 732–742, https://doi.org/10.1016/J.WASMAN.2019.11.019.
[34] Z. Zainal Abidin, S.N.L. Mamauod, A.Z. Romli, S.S. Sarkawi, N.H. Zainal, Synergistic effect of partial replacement of carbon black by palm kernel shell biochar in carboxylated nitrile butadiene rubber composites, Polymers (Basel) (2023) 15, https://doi.org/10.3390/polym15040943.
[35] A. Bardha, S. Prasher, J. Villarta, M.S. Francis, C.Y. Khirpin, J.J. Mehlem, M. J. Dumont, Nut shell and grain husk waste biochar as carbon black replacements in styrene-butadiene rubber composites and improvements through steam activation, Ind. Crops Prod. 203 (2023) 117180, https://doi.org/10.1016/J.INDCROP.2023.117180.
[36] J. Lubura, L. Kobera, S. Abbrent, E. Pavlova, B. Strachota, O. Bera, J. Pavličević, B. Ikonić, P. Kojić, A. Strachota, Natural rubber composites using hydrothermally carbonized hardwood waste biomass as a partial reinforcing filler- part I: structure, morphology, and rheological effects during vulcanization, Polymers (Basel) (2023) 15, https://doi.org/10.3390/polym15051176.
[37] Á. Görbe, A. Kohári, T. Bárány, Rubber compounds from devulcanized ground tire Rubber: recipe formulation and characterization, Polymers (Basel) (2024) 16, https://doi.org/10.3390/polym16040455.
[38] Intergovernmental Panel on Climate Change (IPCC), IPCC Emission Factor Database (EFDB): Carbon Black Production, (2006). https://www.ipcc-nggip.iges.or.jp/efdb/find_ef.php?ipcc_code=2.B.8.f&ipcc_level=3 (accessed August 1, 2025).
[39] K.G. Roberts, B.A. Gloy, S. Joseph, N.R. Scott, J. Lehmann, Life cycle assessment of Biochar systems: estimating the energetic, economic, and climate change potential, Environ. Sci. Technol. 44 (2010) 827–833, https://doi.org/10.1021/es902266r.
[40] EBC (European Biochar Certificate), Certification of the Carbon Sink Potential of Biochar (Version 2.1E), 2021. https://www.european-biochar.org/media/doc/2/c_en_sink-value_2-1.pdf. accessed August 1, 2025.
[41] Accend AS (on behalf of Freres Lumber Co.), Life cycle assessment and calculation of CO_2 removal for Biochar (Version 1.1), Lyons, Oregon, USA, 2021. https://freresswood.com/wpcontent/uploads/2024/04/LCAreportFreresLumberv1.1.pdf (accessed August 1, 2025).
[42] G. Johannesson, S. Boles, L. (editor) Shumaker, GHG Life cycle assessment of CharBoss® biochar production and potential use for CDR certificate generation, Carrboro, NC; Moscow, ID; Portland, OR, USA, 2024. https://biochar-us.org/sites/default/files/presentations/USFS_USBI-CharBoss-LCA-Report-FEB-29-2024-FINAL.pdf (accessed August 1, 2025).
[43] M. Piccioni, F. Martini, C. Martini, C. Toro, Evaluation of energy performance indicators and energy saving opportunities for the Italian rubber manufacturing industry, Energies (Basel) (2024) 17, https://doi.org/10.3390/en17071584.
[44] S. Bakshi, C. Banik, D.A. Laird, Estimating the organic oxygen content of biochar, Sci. Rep. 10 (2020) 13082, https://doi.org/10.1038/s41598-020-69798-y.
[45] D.Y. Kim, J.W. Park, D.Y. Lee, K.H. Seo, Correlation between the crosslink characteristics and mechanical properties of natural rubber compound via accelerators and reinforcement, Polymers (Basel) (2020) 12, https://doi.org/10.3390/polym12092020.
[46] N. Chueangchayaphan, M. Tarasin, W. Phonjon, W. Chueangchayaphan, Evaluating oil palm trunk biochar and palm oil as environmentally friendly sustainable additives in green natural rubber composites, Polymers (Basel) (2025) 17, https://doi.org/10.3390/polym17020223.
[47] L. Li, A. Long, B. Fossum, M. Kaiser, Effects of pyrolysis temperature and feedstock type on biochar characteristics pertinent to soil carbon and soil health: A meta-analysis, Soil Use Manag. 39 (2023) 43–52, https://doi.org/10.1111/sum.12848.
[48] Z.Z. Chowdhury, M.Z. Karim, M.A. Ashraf, K. Khalid, Influence of carbonization temperature on physicochemical properties of biochar derived from slow pyrolysis of durian wood (Durio zibethinus) sawdust, Bioresources 11 (2016) 3356–3372.
[49] M. Cappello, D. Rossi, S. Filippi, P. Cinelli, M. Seggiani, Wood residue-derived biochar as a low-cost, lubricating filler in poly(butylene succinate-co-adipate) biocomposites, Materials (Basel) 16 (2023), https://doi.org/10.3390/ma16020570.
[50] L. Campion, M. Bekchanova, R. Malina, T. Kuppens, The costs and benefits of biochar production and use: A systematic review, J. Clean. Prod. 408 (2023) 137138, https://doi.org/10.1016/J.JCLEPRO.2023.137138.